C. R. Chimie 21 (2018) 247–252

Contents lists available at ScienceDirect

Comptes Rendus Chimie

www.sciencedirect.com

Full paper/Mémoire

Ni–Mo_2C supported on alumina as a substitute for Ni–Mo reduced catalysts supported on alumina material for dry reforming of methane

Lu Yao [a, b], Ye Wang [c], Maria E. Galvez [b], Changwei Hu [a, c, **], Patrick Da Costa [b, *]

[a] Key Laboratory of Green Chemistry and Technology, Ministry of Education, College of Chemistry, Sichuan University, Chengdu, Sichuan, 610064, China
[b] Sorbonne Universités, UPMC, Université Paris-6, Institut Jean-Le-Rond-d'Alembert, 2, place de la Gare-de-Ceinture, 78210 Saint-Cyr-l'École, France
[c] College of Chemical Engineering, Sichuan University, Chengdu, Sichuan 610065, PR China

ARTICLE INFO

Article history:
Received 5 November 2016
Accepted 6 June 2017
Available online 13 July 2017

Keywords:
Methane dry reforming
Carbides
Ni–Mo_2C/Al_2O_3
Stability

ABSTRACT

In this study, alumina-supported Ni–Mo catalysts were carburized to obtain alumina-supported nickel–molybdenum carbides as potential catalysts for dry reforming of methane. The typical carbide was compared with a low carburized material (in 5% H_2/CH_4) and a reduced Ni–Mo catalyst. It was shown that the passivated alumina-supported Ni–Mo catalysts by carbon lead to higher reactivity, selectivity, and stability for dry methane reforming reaction.

1. Introduction

Dry reforming of methane (DRM) has received considerable attention during the past decades as a promising process for the valorization of CO_2 toward the production of synthesis gas [1–3]. Noble metal catalysts (Ru, Rh, Ir, Pd, and Pt) were found to have high catalytic activity for the DRM reaction, but the large-scale application of these catalysts has been limited by their high cost. Thus, Ni-based catalysts were deeply used because they lead to a comparable catalytic activity with high cost-efficiency, but the deactivation was difficult to avoid because of the carbon deposition and Ni^0 sintering [4–7]. Because Levy et al. reported that carbide tungsten displayed reactivity close to that of platinum for neopentane isomerization [9], there has been a large interest in using carbide catalysts. Molybdenum and tungsten carbides (Mo_2C and WC) have been used as the effective catalysts for DRM, partial oxidation, and steam reforming of methane to produce synthesis gas, because Ni-based catalysts seriously suffered from sintering and coking [4–9]. York et al. found that these early transition metal carbides possessed high catalytic activity for methane reforming reactions. On these catalysts, the carbon deposition is lower than reduced Ni-based catalysts because no deactivation was observed at 8 bar [10]. However, at ambient pressure, deactivation was observed because of the conversion of initial Mo_2C to MoO_2 during the reaction. The catalytic activity of the noble and carbide catalysts for methane reforming has been established as follows: Ru > Rh > Ir ≈ Mo_2C > WC > Pd > Pt. Sehested et al. [11] studied Mo_2C catalyst for the DRM reaction at 8 and 1.6 bar total pressure in different reactors. They found that catalysts deactivated from the top to bottom in the plug flow reactor (8 bar) because of the oxidation of the Mo_2C.

* Corresponding author.
** Corresponding author.
E-mail addresses: changweihu@scu.edu.cn (C. Hu), patrick.da_costa@upmc.fr (P. Da Costa).

http://dx.doi.org/10.1016/j.crci.2017.06.002

However, the Mo_2C showed a higher stability at high conversions in the continuously stirred tank reactor (1.6 bar) with no signs of oxidation, but the deactivation was not avoided due to the loss of the surface area of the Mo_2C. Darujati et al. [12] pointed out that both H_2 and CO were found to restrain the oxidation, and this effect could be explained by their influence on the reactions governing carburization and oxidation. The oxidation of the Mo_2C to MoO_2 can be inhibited by feeding CO with the reactants [13]. Although other studies dealt with bulk carbides [14–16] for the DRM reaction, there are only few studies dealing with supported carbides. Brungs et al. [17] found that alumina-supported Mo_2C was stable, and the relative stability of catalysts was as follows: Mo_2C/Al_2O_3 > Mo_2C/ZrO_2 > Mo_2C/SiO_2 > Mo_2C/TiO_2. Natio et al. [18] also reported that supported Mo_2C catalysts were stable and durable for the DRM reaction.

Moreover, Ce promotion on molybdenum carbide catalysts led to an improvement in stability of the catalysts [19,20]. Because Mo_2C species are active for the DRM reaction and Ni-based catalyst would suffer from carbon deposition, carburized Ni–Mo/Al_2O_3 catalyst (Ni–Mo_2C/Al_2O_3 catalyst) was studied for the DRM reaction. In the present work, alumina-supported molybdenum carbide (Mo_2C/Al_2O_3) and alumina-supported nickel–molybdenum carbide (Ni–Mo_2C/Al_2O_3) catalysts were studied for the DRM reaction. To investigate the influence of H_2 concentration on the carburization process and on the performance of the catalyst in the DRM reaction, two different mixtures of H_2/CH_4 ($H_2/CH_4/Ar = 4/20/76$ and $H_2/CH_4 = 80/20$) were used to carburize the precursors. It was shown that the Ni–Mo/Al_2O_3 catalyst carburized by 5% H_2 ($H_2/CH_4/Ar = 4/20/76$) showed the higher catalytic activity for the DRM reaction and that the presence of nickel also promoted the carburization process.

2. Experimental methods

2.1. Preparation of catalyst

The Mo/Al_2O_3 catalyst was synthesized by an incipient wetness impregnation method. Alumina was impregnated with appropriate amounts of $(NH_4)_6Mo_7O_{24}\cdot 4H_2O$ solution corresponding to a nominal Mo loads of 10 wt %. After 2 h of impregnation, the excess solvent (deionized water) was removed by rotary evaporator at 60 °C. Then the obtained sample was dried at 110 °C overnight and calcined in synthetic air at 550 °C for 4 h. With the similar method, alumina was impregnated with appropriate amounts of $(NH_4)_6Mo_7O_{24}\cdot 4H_2O$ and $Ni(NO_3)_2\cdot 6H_2O$ mixed solution, corresponding to nominal Ni and Mo loadings of 10 wt %, leading to the Ni–Mo/Al_2O_3 catalyst.

Mo/Al_2O_3 and Ni–Mo/Al_2O_3 catalysts were thus carburized by the temperature-programmed process in H_2/CH_4 ($F_{H_2} = 40$ mL/min and $F_{CH_4} = 10$ mL/min) to obtain the Mo_2C/Al_2O_3 and Ni–Mo_2C/Al_2O_3 catalysts, respectively. To investigate the influence of H_2 concentration on the carburization process and on the performance of the catalyst in the DRM reaction, two different mixtures of H_2/CH_4 (5%H_2 and pure H_2) were used to carburize the catalyst precursors.

The first one consisted of used 5%H_2 (argon as balance), and the total ratio was kept 40/10, but the H_2/CH_4 becomes 2/10 because of the use of dilute H_2, that is, $H_2/CH_4/Ar = 4/20/76$. This synthesis has led to a reduced material with a passivation surface of carbon. The second one consisted of a feed with pure hydrogen and pure methane in a ratio of 40/10, that is, $H_2/CH_4 = 80/20$. The 5% H_2/CH_4 carbide Mo/Al_2O_3, 5% H_2/CH_4 carbide Ni–Mo/Al_2O_3, pure H_2/CH_4 carbide Mo/Al_2O_3, and pure H_2/CH_4 carbide Ni–Mo/Al_2O_3 catalysts were named as MC-1, NMC-1, MC-2, and NMC-2, respectively.

For both carburization processes, temperature-programmed process was used as following: temperature was raised from room temperature (around 25 °C) to 300 °C at a rate of 5 °C/min in H_2/CH_4 mixture, then from 300 °C to 700 °C at a rate of 1 °C/min (H_2/CH_4 mixture), after that kept at 700 °C for 2 h (H_2/CH_4 mixture), and then cooled down to room temperature overnight in Ar. After carburization, the catalyst was passivated in a CO_2 atmosphere at room temperature to be characterized or directly tested without passivation or reduction in the DRM reaction.

2.2. Catalytic activity test

DRM activity experiments were carried out over reduced and carbide catalysts. DRM activity experiments of reduced samples were carried out in a tubular quartz reactor at atmospheric pressure using a $CH_4/CO_2/Ar = 1/1/8$ mixture, at temperatures from 850 to 550 °C. Before the catalytic activity test, the catalysts were reduced in situ at 900 °C in 5% H_2–Ar for 1 h. For stability tests, catalysts were reduced at 900 °C for 1 h and then cooled down to 700 °C to carry out the DRM reaction for 300 min.

DRM activity experiments on carburized catalysts were carried out in the similar way. After the carburization, catalysts were directly heated up in Ar to 850 °C to perform the DRM reaction without any prior reduction. For stability tests, the carbide catalysts were directly heated up in Ar to 700 °C to carry out the DRM reaction during 300 min.

For all the catalytic tests, the gas hourly space velocity was kept as 20,000 h^{-1}. The effluent was analyzed in a microgas chromatograph (Varian CPi 4900) online, equipped with COX column. Methane and CO_2 conversions, as well as the H_2/CO ratio, were calculated using the molar composition of both the reactant mixture and the gas exiting the catalytic reactor, determined by gas chromatography.

2.3. Characterization

Nitrogen adsorption isotherms were acquired at −196 °C in an ASAP 2020 device, upon degasification of the materials at 250 °C. The carbide catalysts were analyzed by inductively coupled plasma (ICP, ARCOS) to determine the nominal amounts of Ni and Mo. The Ni and Mo species were extracted by dilute hydrochloric acid, at 80 °C under reflux for 5 h before ICP analysis. The X-ray diffraction (XRD) patterns were obtained using a PANalytical-Empyrean diffractometer, equipped with a Cu Kα (λ =

1.5406 Å) radiation source. The data were collected with a step of 0.02°/s.

X-ray photoelectron spectroscopy (XPS) experiment was performed on an AXIS Ultra DLD (KRATOS) spectrometer using Al Kα radiation (1486.6 eV) operated at an accelerating power of 150 W. The binding energy (BE) was calibrated using C 1s at 284.6 eV.

3. Results and discussion

3.1. Catalytic activity for DRM over carbide catalysts versus reduced ones

Tables 1–3 present the values of the steady-state methane and CO_2 conversions, as well as H_2/CO ratio measured during the DRM catalytic activity experiment. It can be seen that both the reduced Mo/Al_2O_3 and MC-1 showed very low methane and CO_2 conversions. Even at 700 °C, the conversions of CO_2 were 10.9% and 6.3% for Mo/Al_2O_3 and MC-1 catalysts, respectively. It is well known that molybdenum alone is not an efficient catalyst for DRM [21]. When a carburization in pure H_2 is conducted (MC-2) the catalytic results are even worse (3% conversion at 700 °C) (results not shown).

When nickel is added, that is, for $Ni–Mo/Al_2O_3$ reduced or carbide catalysts, the catalytic activity was found to be much higher than that in the absence of nickel. At 700 °C, the conversions of CO_2 were 35.7% and 38.1% for reduced $Ni–Mo/Al_2O_3$ and NMC-1 catalysts, respectively. It is well known that Ni^0 is the active phase in DRM reactions [22,23].

In Table 1, all the CO_2 conversions of the NMC-1 catalyst were higher than those of both reduced $Ni–Mo/Al_2O_3$ and NMC-2 (except at 800 °C), especially at 900 °C. At 900 °C, CO_2 conversion of the NMC-1 catalyst was 7.2% higher than that of the NMC-2 catalyst, which may be attributed to the reaction of CO_2 with the surface carbon formed during carburization (5% H_2/CH_4) on NMC-1.

Table 2 shows that, at 850 and 800 °C, CH_4 conversions of NMC-1 were 89.9% and 78.6%, respectively, which are slightly lower than those of the reduced $Ni–Mo/Al_2O_3$ catalyst. Although CH_4 conversion of NMC-1 was higher

Table 1
Steady-state CO_2 conversions of the catalysts for DRM.

Catalyst	CO_2 conversions at different reaction temperatures (%)						
	850 °C	800 °C	750 °C	700 °C	650 °C	600 °C	550 °C
Reduced Mo/Al_2O_3	58.5	35.0	19.6	10.9	5.6	2.4	0.4
MC-1	51.4	31.1	18.7	6.3	2.1	0	0
Reduced $Ni–Mo/Al_2O_3$	93.4	85.0	71.6	53.5	35.7	18.9	7.9
NMC-1	99.2	84.3	72.4	54.9	38.1	21.9	10.6
NMC-2	78.5	78.2	62.1	45.9	28.1	14.9	0.5

Table 2
Steady-state CH_4 conversions of the catalysts for DRM.

Catalyst	CH_4 conversions at different reaction temperatures (%)						
	850 °C	800 °C	750 °C	700 °C	650 °C	600 °C	550 °C
Reduced Mo/Al_2O_3	52.9	29.4	17.7	11.4	8.0	6.1	5.0
MC-1	40.9	25.9	15.4	5.7	2.4	1.5	1.2
Reduced $Ni–Mo/Al_2O_3$	91.1	79.8	63.7	45.1	27.6	14.1	6.4
NMC-1	89.9	78.6	64.4	46.7	29.4	16.1	7.4
NMC-2	79.2	73.0	59.0	43.3	27.5	13.9	2.0

Table 3
H_2/CO ratio for the studied catalysts for DRM.

Catalyst	Ratio of H_2/CO						
	850 °C	800 °C	750 °C	700 °C	650 °C	600 °C	550 °C
Reduced Mo/Al_2O_3	0.76	0.65	0.56	0.49	0.41	0.33	0.25
MC-1	0.77	0.73	0.67	0.50	0.31	0.21	0.19
Reduced $Ni–Mo/Al_2O_3$	0.93	0.89	0.82	0.74	0.65	0.53	0.40
NMC-1	0.92	0.89	0.83	0.75	0.65	0.54	0.40
NMC-2	0.94	0.92	0.88	0.86	0.83	0.74	0.30

than that of NMC-2 at 850 and 800 °C, respectively, at lower temperature (750, 700, 650, 600 and 550 °C), all the CH_4 conversions of NMC-1 were higher than those of both reduced Ni–Mo/Al_2O_3 and NMC-1catalysts. Finally, the H_2/CO ratio for the NMC-1 catalyst was similar to that obtained for the reduced Ni–Mo/Al_2O_3 catalyst (Table 3).

3.2. Stability of NCM-1 versus reduced Ni–Mo/Al_2O_3 catalyst

For reduced Ni–Mo/Al_2O_3 catalyst, the initial conversion of CH_4 (39.9%) was lower than that of the NMC-1 catalyst (41.7%). At 300 min, CH_4 conversion of the reduced Ni–Mo/Al_2O_3 catalyst decreased to 36.8%. However, for the NMC-1 catalyst, no deactivation is observed because CH_4 conversion remains almost constant after 300 min, with around 1% of conversion decrease. Comparing to initial CO_2 conversion, CO_2 conversion of the reduced Ni–Mo/Al_2O_3 catalyst decreases (16.5% less) after 300 min, whereas for NMC-1, for CO_2 conversion only 8.7% of decrease is observed. Thus, in addition to the improvement in the catalytic activity, the stability after 300 min of NMC-1 is also enhanced.

3.3. Carbides' characterization and relations with catalytic activity

The Brunauer, Emmett et Teller (BET) surface area, pore volume, and mean pore size, obtained from the N_2 adsorption isotherms acquired for the Ni and Mo–Ni catalysts are presented in Table 4. The BET surface area slightly decreases for NMC catalysts compared with MC catalyst. These results can be explained by the addition of Ni to the Mo/Al_2O_3 catalyst.

The average pore size range was found from 7.7 to 8.3 nm. As a consequence of pore blockage, occurring with loadings of 10 wt % Ni and 10 wt % Mo, the Ni–Mo/Al_2O_3 catalyst shows the lowest surface area and total pore volume of the catalysts series. Nevertheless, the textural properties of the different catalysts remain very similar, with this loss of surface area due to partial pore blockage in Ni–Mo/Al_2O_3 with a decrease of 10% with respect to the monometallic Ni catalyst (Fig. 1).

Fig. 2 presents the XRD patterns of the Mo-bearing catalysts after carburization.

No diffraction peaks of Mo_2C species were observed on all the carbide catalysts because of the low loading of molybdenum or the highly dispersed state of the carbide phase. Moreover, neither metallic Ni nor graphitic species are observed on carbide Mo/Al_2O_3 (both MC-1 and MC-2) and NMC-2. However, for the NMC-1, both diffraction peaks of graphitic C and metallic Ni are observed. The presence of Ni^0 can then be linked directly with the higher activity found for such catalysts in the DRM reaction. Moreover, the graphitic carbon would avoid the C deposition during the DRM reaction and then would lead to a higher stability of NMC-1. Finally, the presence of diffraction peaks of graphitic C indicates that the presence of Ni

Table 4
Textural properties: BET surface area, total pore volume, and mean pore size, Ni–Mo catalysts.

Catalyst	BET surface area (m^2/g)	Pore volume (cm^3/g)	Pore size (nm)
Mo/Al_2O_3 (**reduced**)	170.1	0.30	8.3
Ni–Mo/Al_2O_3 (**reduced**)	156.1	0.30	7.7
NMC-1	153.1	0.28	7.3
NMC-2	154.1	0.29	7.4

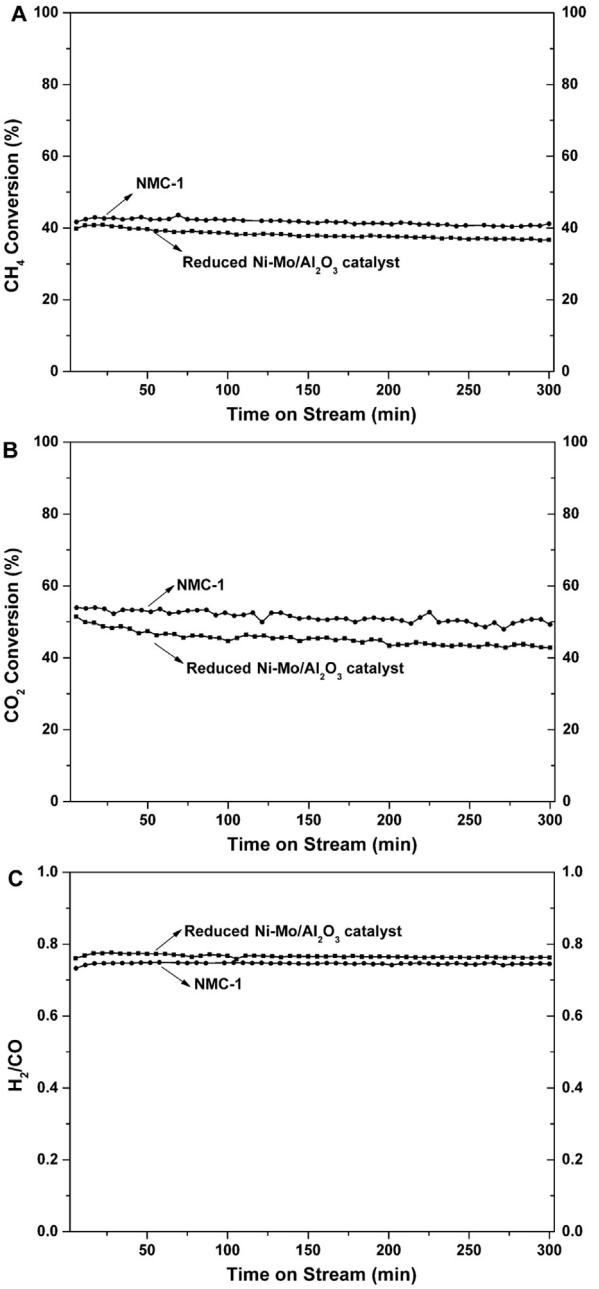

Fig. 1. DRM catalytic test results of reduced Ni–Mo/Al_2O_3 and NMC-1 for 300 min at 700 °C: (A) CH_4 conversions, (B) CO_2 conversions, and (C) H_2/CO ratios.

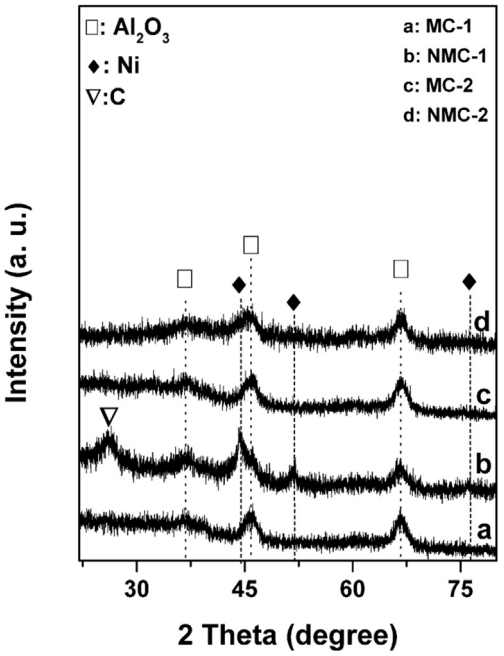

Fig. 2. XRD patterns of the carbide catalysts.

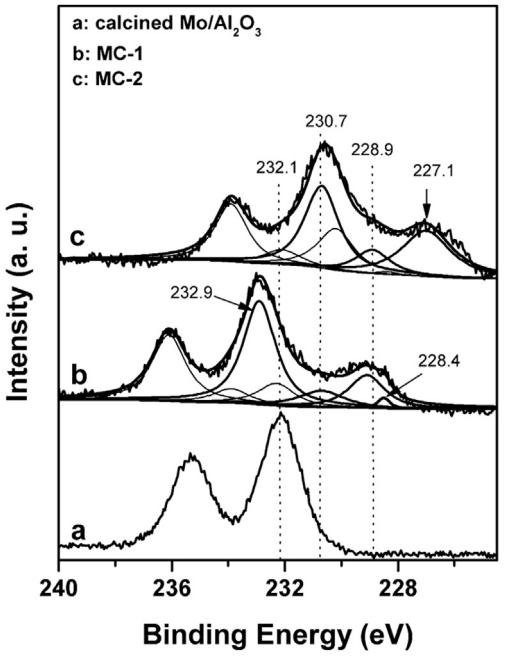

Fig. 3. XPS spectra of Mo 3d of Mo catalysts.

facilitated the carburization process and the decomposition of CH_4.

Table 5 shows the content of metals in carbide catalysts according to ICP results. It can be seen that the content of Ni and Mo was lower than 10%, which may be because of the formation of Mo_2C or deposited carbon on the surface. Table 5 also shows that there was a lowest amount of Mo and Ni in NMC-1, which may be because of a better carburization or more carbon formation on the surface of the catalysts The ICP results are in good agreement with that XR diffractograms.

Fig. 3 shows XPS spectra of Mo 3d of the Mo/Al_2O_3 catalyst. The doublet peaks of Mo 3d have a splitting of 3.2 eV and the ratio of $3d_{5/2}/3d_{3/2}$ of 3:2 was considered. Through deconvolution, the distribution of molybdenum oxidation states was estimated, and the Mo $3d_{5/2}$ BE and the ratio of surface carbide molybdenum species to total molybdenum species denoted as $Mo^{2+}/(Mo^{0+} + Mo^{2+} + Mo^{4+} + Mo^{5+} + Mo^{6+})$ are shown in Table 6. The peak with BE of 228.2 eV was assigned to Mo^{2+} species involved in Mo—C bonding [15,24,25]. The others peaks with $3d_{5/2}$ BE of 227.1, 228.9, 232.9, and 230.7 eV are attributed to metallic Mo^0, Mo^{4+}, Mo^{5+}, and Mo^{6+} species, respectively [15,24,25]. On can conclude that the Mo species in the calcined Mo/Al_2O_3 catalyst are mainly in the form of Mo^{6+}, whereas after carburization in pure H_2/CH_4, there were at least three molybdenum species on the carbide MC-2 catalyst.

Table 5
The amount of metals in carbide catalysts according to ICP results.

Catalyst	Mo (wt %)	Ni (wt %)
MC-1	6.3	–
MC-2	7.2	–
NMC-1	4.2	5.0
NMC-2	7.5	8.1

Almost no carbide molybdenum was detected on MC-2. The presence of the higher oxidation state molybdenum may be because of (1) the oxidation of the surface molybdenum species during the passivation process after carburization, (2) the oxidation of the surface molybdenum species when the catalyst was exposed to air, and (3) the incomplete carburization [15,26]. However, when using the 5% H_2 instead of pure H_2 to carburize the Mo/Al_2O_3 catalyst (MC-1), the Mo^{2+} species (Mo_2C) was detected with the ratio of $Mo^{2+}/(Mo^{0+} + Mo^{2+} + Mo^{4+} + Mo^{5+} + Mo^{6+})$ of 2.5%. From the aforementioned results, it could be deduced that Mo_2C phase is formed preferentially in dilute H_2/CH_4 than that in pure H_2/CH_4.

XPS spectra of Mo 3d of Ni—Mo catalysts are presented in Fig. 4. The Mo $3d_{5/2}$ BE was centered at 231.2 eV in the calcined Ni—Mo/Al_2O_3 catalyst, which corresponds to a 0.9 eV shift to the lower BE compared with that of the calcined Mo/Al_2O_3 catalyst. This result suggests that the presence of Ni enhances the electron density around Mo. After carburizing in pure H_2/CH_4, five molybdenum species on NMC-2 can be identified. These are Mo^0, Mo^{2+}, Mo^{4+}, Mo^{5+}, and Mo^{6+} species, and the ratio of $Mo^{2+}/(Mo^{0+} + Mo^{2+} + Mo^{4+} + Mo^{5+} + Mo^{6+})$ was 13.3%. On the contrary, on NMC-1, no Mo^0 was detected, and the $Mo^{2+}/(Mo^{0+} + Mo^{2+} + Mo^{4+} + Mo^{5+} + Mo^{6+})$ ratio is 22.8%. Furthermore, the aforementioned results indicate that different surface carbon species were formed on the carbide catalysts during the carburization process. Thus, during the pure H_2/CH_4 carburization process, some molybdenum may be over reduced to Mo^{0+} instead of Mo^{2+} (Mo_2C), which led to a lower ratio of $Mo^{2+}/(Mo^{0+} + Mo^{2+} + Mo^{4+} + Mo^{5+} + Mo^{6+})$. The aforementioned results show that the presence

Table 6
Mo $3d_{5/2}$ binding energy and $Mo^{2+}/(Mo^{0+} + Mo^{2+} + Mo^{4+} + Mo^{5+} + Mo^{6})$ ratios of the carbide catalysts.

Catalysts	Mo $3d_{5/2}$ (eV)					$Mo^{2+}/(Mo^{0+} + Mo^{2+} + Mo^{4+} + Mo^{5+} + Mo^{6+})$ (%)
	Mo^0 (metallic)	Mo^{2+} (carbide)	Mo^{4+} (oxide)	Mo^{5+} (oxide)	Mo^{6+} (oxide)	
MC-1	–	228.4	229.1	230.7	232.9	2.5
MC-2	227.1	–	228.9	230.7	–	0
NMC-1	–	228.4	228.9	230.5	233.0	22.8
NMC-2	227.3	228.2	228.9	230.9	232.1	13.3

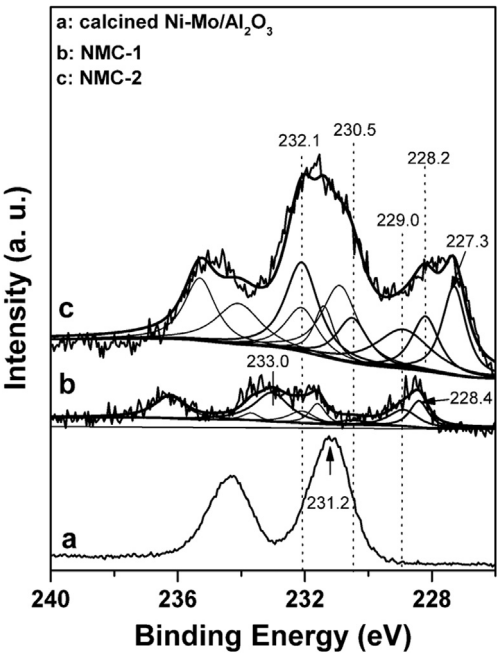

Fig. 4. XPS spectra of Mo 3d of Ni–Mo catalysts.

of nickel promoted the carburization process, and this statement is also in good agreement with the literature [15,27]. Finally, the aforementioned XPS results in which NMC-1 exhibited highest amount of Mo_2C species are also in line with the activity test results that the NMC-1 showed the best catalytic activity for the DRM reaction.

4. Conclusions

Alumina-supported Ni–Mo carbides (Ni–Mo_2C) were chosen as a substitute for the alumina-supported Ni–Mo reduced catalyst for DRM. We clearly showed that the presence of nickel promoted the carburization process. It was also proved that a Mo_2C phase is preferentially formed under dilute H_2/CH_4 (5%H_2/pure CH_4) than that in pure H_2/CH_4 (pure H_2/pure CH_4). Moreover, by XRD, we clearly also found that graphitic C (or passivated C) and metallic Ni^0 were only present on the NMC-1 (5%H_2/pure CH_4 carbide). Thus, it is easy to conclude that NMC-1 (5%H_2/pure CH_4 carbide) was found to be a more active and more stable catalyst than that of the reduced Ni–Mo/Al_2O_3 catalyst for the DRM reaction.

Acknowledgments

L.Y. is grateful to the Chinese Scholarship Council (CSC) and National Natural Science Foundation of China (21321061) for the financial support.

References

[1] R. Benraba, A. Löfberg, J. Guerrero Caballero, E. Bordes-Richard, A. Rubbens, R.-N. Vannier, H. Boukhlouf, A. Barama, Catal. Commun. 58 (2015) 127–131.
[2] S.A. Theofanidis, R. Batchu, V.V. Galvita, H. Poelman, G.B. Marin, Appl. Catal., B 185 (2016) 42–55.
[3] B.A. Rosen, E. Gileadi, N. Eliaz, Catal. Commun. 76 (2016) 23–28.
[4] Z. Hou, J. Gao, J. Guo, D. Liang, H. Lou, X. Zheng, J. Catal. 250 (2007) 331–341.
[5] Z. Li, Y. Kathiraser, S. Kawi, ChemCatChem 7 (2015) 160–168.
[6] H. Düdder, K. Kähler, B. Krause, K. Mette, S. Kühl, M. Behrens, V. Scherer, M. Muhler, Catal. Sci. Technol. 4 (2014) 3317–3328.
[7] A.G. Bhavani, W.Y. Kim, J.Y. Kim, J.S. Lee, Appl. Catal., A 450 (2013) 63–72.
[8] M.L. Pritchard, R.L. McCauley, B.N. Gallaher, W.J. Thomson, Appl. Catal., A 275 (2004) 213–220.
[9] R.B. Levy, M. Boudart, Science 181 (1973) 547–549.
[10] A.P.E. York, J.B. Claridge, A.J. Brungs, S.C. Tsang, M.L.H. Green, Chem. Commun. (1997) 39–40.
[11] J. Sehested, C.J.H. Jacobsen, S. Rokni, J.R. Rostrup-Nielsen, J. Catal. 201 (2001) 206–212.
[12] A.R.S. Darujati, D.C. LaMont, W.J. Thomson, Appl. Catal., A 253 (2003) 397–407.
[13] D.C. LaMont, W.J. Thomson, Chem. Eng. Sci. 60 (2005) 3553–3559.
[14] A. Zhang, A. Zhu, B. Chen, S. Zhang, C. Au, C. Shi, Catal. Commun. 12 (2011) 803–807.
[15] C. Shi, A. Zhang, X. Li, S. Zhang, A. Zhu, Y. Ma, C. Au, Appl. Catal., A 431–432 (2012) 164–170.
[16] S. Zhang, C. Shi, B. Chen, Y. Zhang, Y. Zhu, J. Qiu, C. Au, Catal. Today 258 (2015) 676–683.
[17] A.J. Brungs, A.P.E. York, J.B. Claridge, C.M. Arquez-Alvarez, M.L.H. Green, Catal. Lett. 70 (2000) 117–122.
[18] S. Naito, M. Tsuji, T. Miyao, Catal. Today 77 (2002) 161–165.
[19] A.R.S. Darujati, W.J. Thomson, Appl. Catal., A 296 (2005) 139–147.
[20] A.R.S. Darujati, W.J. Thomson, Chem. Eng. Sci. 61 (2006) 4309–4315.
[21] M. Gaillard, M. Virginie, A.Y. Khodakov, Catal. Today 261 (2016) 137–145.
[22] Z. Shang, S. Li, L. Li, G. Liu, X. Liang, Appl. Catal., B 201 (2017) 302–309.
[23] Y. Chen, J. Ren, Catal. Lett. 29 (1994) 39–48.
[24] X. Huo, Z. Wang, J. Huang, R. Zhang, Y. Fang, Catal. Commun. 79 (2016) 39–44.
[25] C. Shi, S. Zhang, X. Li, A. Zhang, M. Shi, Y. Zhu, J. Qiu, C. Au, Catal. Today 233 (2014) 46–52.
[26] J. Patt, D.J. Moon, C. Phillips, L. Thompson, Catal. Lett. 65 (2000) 193–195.
[27] N. Ji, T. Zhang, M. Zheng, A. Wang, H. Wang, J.G. Chen, Angew. Chem., Int. Ed. 47 (2008) 8510–8513.